the most favorable process, theoretical studies by Gordon and co-workers[62] suggest that the 1,2-elimination process has a higher activation barrier than a 1,1-elimination process. As a result, the direct formation of silaethylenes in the pyrolysis of silanes under homogeneous conditions is unlikely. The $\Delta H°$ values for 1,1-elimination of hydrogen in the pyrolysis of SiH_4,[56] CH_3SiH_3,[57,58] and $(CH_3)_2SiH_2$[57,59] are almost identical, but the E_a values tend to increase by ~4.2 kcal/mol per methyl group with increasing methyl substitution in place of hydrogen. The E_a values for 1,1-elimination of methane in the pyrolysis of CH_3SiH_3 and $(CH_3)_2SiH_2$ are slightly higher than those for 1,1-elimination of hydrogen and increase as a result of methyl substitution by ~6.7 kcal/mol per methyl group. This may indicate that methyl substitution at the silicon center in silylenes raises the activation energy for insertion into H-H or C-H bonds by ~4.2 or ~6.7 kcal/mol, respectively.[59] The pyrolysis mechanism of trimethylsilane[60] has not been well established because of the complexity of the mechanism and the lack of experimental data for most of its steps. It will be of particular interest to see if the pyrolysis of trimethylsilane involves a 1,1-elimination process to form $Si(CH_3)_2$. For this process, estimates of Arrhenius parameters are ~14.8 and ~80 kcal/mol for log A and E_a by analogy with pyrolysis reactions of CH_3SiH_3 and $(CH_3)_2SiH_2$. In the pyrolysis of tetramethylsilane, Davidson and co-workers[60] concluded that the formation of methane at high temperature (955-1055 K) relates to a nonchain mechanism rate-determined by the Si-C bond rupture process with E_a of 84.8 kcal/mol, while at low temperature (840-950 K), a short-chain sequence probably operates. This may indicate that the molecular process involving 1,2-elimination of methane or 1,1-elimination of ethane in the pyrolysis of tetramethylsilane requires a higher activation energy than the Si-C bond rupture process.

A Study of the Thermal Decomposition and Dehydrochlorination of *N*-Chloroazetidine: Microwave Spectra of *N*-Chloromethylenimine, 1-Azetine, and 2-Azabutadiene

Masaaki Sugie,* Harutoshi Takeo, and Chi Matsumura

Contribution from the National Chemical Laboratory for Industry, Tsukuba, Ibaraki, 305 Japan.
Received June 22, 1988

Abstract: The microwave spectrum of *N*-chloromethylenimine and 1-azetine has been observed following pyrolysis and dehydrochlorination of *N*-chloroazetidine, respectively. In addition, pyrolysis of 1-azetine gives another unstable molecule, 2-azabutadiene. The rotational constants determined are A = 62434.90 (10), B = 6676.389 (13), and C = 6022.843 (11) MHz for *N*-chloromethylenimine, A = 62344.73 (11), B = 6531.700 (13), and C = 5904.017 (11) MHz for the ^{37}Cl species of *N*-chloromethylenimine, A = 13911.630 (24), B = 12713.799 (24), and C = 7254.990 (24) MHz for 1-azetine, and A = 47186.010 (23), B = 4886.5325 (27), and C = 4430.0673 (23) MHz for 2-azabutadiene. The dipole moments and nuclear quadrupole coupling constants have also been determined from analysis of the spectra. The molecular constants estimated by ab initio MO calculations have been found to be consistent with the experimental results.

We studied the pyrolysis of 2-methylaziridine (**1**; in Figure 1) in the gas phase by microwave spectroscopy[1] and found a new transient molecule *N*-methylvinylamine (**2**), which was unstable and easily rearranged to its tautomer *N*-methylethylidenimine (**3**). Recently, it has been found[2] that the pyrolysis of *N*-chloro-2-methylaziridine (**4**) gives unstable molecules, *N*-methylketenimine (**5**) and 2-methylazirine (**6**). Amatatsu et al.[3,4] studied the same reaction systems by infrared spectroscopy and identified similar reaction products as observed by us. These experimental results show that there exist more than two reaction pathways for 3-membered ring systems containing a chlorine atom. The ring cleavage is facile at elevated temperatures since a 3-membered ring molecule has a high ring strain. The resultant reactive intermediate is stabilized by hydrogen rearrangement. The dehydrohalogenation is another pathway and is as probable as the ring cleavage.

As for 4-membered ring systems, it is well-known[5] that azetidine (**7**) cleaves into ethylene and methylenimine (**8**). We have studied the pyrolysis of *N*-chloroazetidine (**9**) by microwave spectroscopy and found that the reaction is similar to that of azetidine. That is, the microwave spectrum of *N*-chloromethylenimine (**10**) was observed as one of the pyrolysis products.

Guillemin et al.[6] obtained 1-azetine (**11**) by dehydrochlorination of *N*-chloroazetidine. They obtained structural proof by such chemical procedures as reduction by $LiAlH_4$ and addition of HCN. Physical proofs were obtained by infrared, ^1H NMR, and ^{13}C NMR spectra. They also found that 2-azabutadiene (**12**) was produced by the flash vacuum photolysis of 1-azetine.

We obtained the microwave spectra of 1-azetine and 2-azabutadiene by a similar method, and the analysis of the spectra is presented together with that of *N*-chloromethylenimine.

The ab initio MO calculation was used as an aid to the analysis of spectra and the confirmation of the molecules. The results of ab initio MO calculations are also presented.

Experimental Section

A precursor sample, *N*-chloroazetidine, was prepared by passing azetidine through a U-tube containing NCS (*N*-chlorosuccinimide). The mixture containing azetidine and chloride was introduced into a 3-m X-band waveguide cell through a 4-mm i.d. quartz tube heated to about 600 °C, and the microwave spectrum of *N*-chloromethylenimine was observed. The spectrum of 1-azetine was obtained by passing *N*-chloroazetidine through a second U-tube, which contained *t*-BuOK (potassium tertiary butylate). This U-tube was heated to about 80 °C in order to maintain a high reaction efficiency. In order to observe the spectrum of 2-azabutadiene, the gas mixture emerging from the second U-tube was passed through the quartz tube heated to about 650 °C and introduced into the waveguide cell. A fast-flow method was adopted since

(1) Sugie, M.; Takeo, H.; Matsumura, C. *Chem. Phys. Lett.* **1985**, *113*, 140-144.
(2) Sugie, M.; Takeo, H.; Matsumura, C., to be submitted for publication.
(3) Amatatsu, Y.; Hamada, Y.; Tsuboi, M.; Sugie, M. *J. Mol. Spectrosc.* **1985**, *111*, 29-41.
(4) Amatatsu, Y.; Hamada, Y.; Tsuboi, M. *J. Mol. Spectrosc.* **1987**, *123*, 476-485.
(5) Rodler, M.; Bauder, A. *J. Mol. Struct.* **1983**, *97*, 47-52.
(6) Guillemin, J. C.; Denis, J. M.; Lablache-Combier, A. *J. Am. Chem. Soc.* **1981**, *103*, 468-469.

0002-7863/89/1511-0906$01.50/0

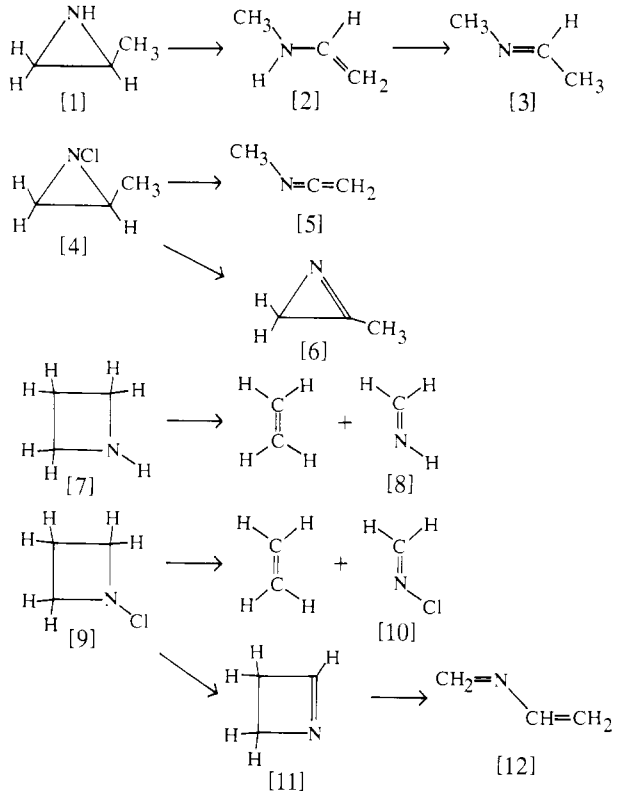

Figure 1. Reaction of methylaziridine, azetidine, and their chlorine derivatives.

the lifetimes of *N*-chloromethylenimine, 1-azetine, and 2-azabutadiene in the brass waveguide cell were about 10, 2, and 1 min, respectively.

Microwave spectra were obtained with a conventional 100-kHz Stark modulation spectrometer controlled by an NEC PC9801m microcomputer. The microwave sources were an HP 8672A synthesized signal generator for 8–18 GHz, the signal generator with a frequency doubler for 18–27 GHz, and an HP 8690B sweep oscillator with two plug-in RF units, which was phase-locked to the synthesized signal generator for 27–50 GHz, and an OKI klystron 50V11, which was also phase-locked to the synthesizer for the region higher than 50 GHz. The measured frequency range was 8–52 GHz. The scanning of frequency was made by the microcomputer through an HP-IB interface. The output signal of the spectrometer was also processed by the microcomputer through an A/D converter, and thereby the center frequencies of the spectral lines were automatically measured. The uncertainties of the transition frequencies thus obtained are less than 0.1 MHz. Some of the transitions exhibit broad spectral features, owing to unresolved nuclear quadrupole interaction. The uncertainties of such transitions amount to 0.2 MHz at most. The spectra were observed with the cell temperature at about −20 °C. The pressure of the sample in the cell was about 10–20 mTorr.

Ab Initio MO Calculation. Ab initio MO calculations were performed to estimate the geometrical structures, dipole moments, and nuclear quadrupole coupling constants. The program HONDOG was used. This program was originally written by Dupuis and King[7] and modified at the Institute for Molecular Science, Okazaki, Japan. The nuclear quadrupole coupling constants were calculated from the field gradients. This part of the program was written by Yamanouchi.[8] Calculations were carried out on the IBM 3081K computer system in the Tsukuba Research Center.

A 4-31G* basis set was used for *N*-chloromethylenimine, while 4-31G(N*) basis sets were used for 1-azetine and 2-azabutadiene. The fully optimized geometries are given in Tables I–III. The rotational constants and dipole moments calculated from the optimized geometries are also listed in the tables.

Analysis of the Spectrum. *N*-Chloromethylenimine. The ab initio MO calculation using a 4-31G* basis set showed that *N*-chloromethylenimine has large a and b components of the dipole moment. Therefore, a-type R-branch transitions were first searched for in the frequency region estimated from the calculated rotational constants. The strong a-type R-branch $J = 3 \leftarrow 2$ transitions were easily identified from their characteristic Stark patterns. The a-type R-branch transitions of $J = 2 \leftarrow 1$ and $1 \leftarrow 0$ were successively identified in the neighborhood of the frequency region estimated from the $J = 3 \leftarrow 2$ transitions. These transitions showed hyperfine structures due to the nuclear quadrupoles of chlorine and nitrogen atoms, and the splittings amount to 30 MHz at most. These hyperfine patterns were well explained by the quadrupole coupling constants of the chlorine calculated by the ab initio MO calculation. Such a-type Q-branch transitions as $10_{1,9}$–$10_{1,10}$, $11_{1,10}$–$11_{1,11}$ were expected to show doublets, the spacing of which is about 3 MHz. These Q-branch transitions were carefully searched for with the approximate rotational constants which are determined by R-branch transitions and were found successfully.

As for the b-type transitions, a series of $(J-1)_{2,J-3}$–$J_{1,J}$ transitions were first found, since they were expected to show doublets of about 3 MHz.

Table I. Calculated Molecular Structure and Molecular Constants of *N*-Chloromethylenimine[a]

	bond length, Å		bond angle, deg
C=N	1.248	∠CNCl	114.4
N–Cl	1.720	$\angle NCH_4$	124.7
$C–H_4$	1.078	$\angle NCH_5$	116.4
$C–H_5$	1.077		
	rotational constant, MHz		dipole moment, D
A	66532	μ_a	1.95
B	6769	μ_b	1.90
C	6144	μ_c	0.0

[a] Atoms are numbered as follows:

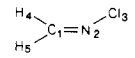

Table II. Calculated Molecular Structure and Molecular Constants of 1-Azetine[a]

	bond length, Å		bond angle, deg
$C_1–C_2$	1.510	∠CC=N	99.5
$C_1–C_4$	1.563	∠C=NC	91.9
C=N	1.264	∠CCC	88.2
C–N	1.489	∠CCN	80.5
$C–H_5$	1.080	$\angle C_2C_1H_5$	116.3
$C–H_7$	1.073	$\angle C_1C_2H_7$	133.3
$C–H_8$	1.080	$\angle C_1C_4H_8$	116.0
	rotational constant, MHz		dipole moment, D
A	14078	μ_a	2.26
B	12918	μ_b	1.13
C	7350	μ_c	0.0

[a] Atoms are numbered as follows:

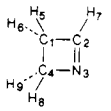

Table III. Calculated Molecular Structure and Molecular Constants of 2-Azabutadiene[a]

	bond length, Å		bond angle, deg
C=C	1.318	∠C=CN	120.7
C=N	1.254	∠CN=C	118.6
C–C	1.409	$\angle C=CH_5$	121.7
$C–H_5$	1.071	$\angle C=CH_6$	120.8
$C–H_6$	1.071	$\angle C=CH_7$	121.0
$C–H_7$	1.079	$\angle N=CH_8$	124.1
$C–H_8$	1.081	$\angle N=CH_9$	119.5
$C–H_9$	1.075		
	rotational constant, MHz		dipole moment, D
A	49086	μ_a	0.42
B	4926	μ_b	1.64
C	4477	μ_c	0.0

[a] Atoms are numbered as follows:

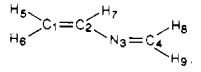

(7) Dupuis, M.; King, H. F. *J. Chem. Phys.* **1978**, *68*, 3998–4004.
(8) Yamanouchi, K.; Sugie, M.; Takeo, H.; Matsumura, C.; Kuchitsu, K. *J. Mol. Struct.* **1985**, *126*, 321–330.

Table IV. Transition Frequencies of *N*-Chloromethylenimine

transition	$CH_2N^{35}Cl$ ν_{obs}[a]	$CH_2N^{35}Cl$ Δ[b]	$CH_2N^{37}Cl$ ν_{obs}[a]	$CH_2N^{37}Cl$ Δ[b]
a-Type				
$1_{0,1}-0_{0,0}$	12699.21	−0.01	12435.78	0.08
$2_{0,2}-1_{0,1}$			24866.05	0.00
$2_{1,2}-1_{1,1}$	24745.07	0.09		
$2_{1,1}-1_{1,0}$	26051.79	−0.03	25498.87	−0.06
$3_{0,3}-2_{0,2}$	38074.53	0.10	37285.74	0.05
$3_{1,3}-2_{1,2}$	37113.78	0.07	36362.20	−0.05
$3_{1,2}-2_{1,1}$	39073.87	−0.01	38244.85	0.01
$3_{2,1}-2_{2,0}$	38120.44	−0.03	37328.08	−0.07
$4_{0,4}-3_{0,3}$	50738.84	−0.01	49689.29	−0.01
$4_{1,4}-3_{1,3}$	49477.87	−0.10	48476.60	0.05
$4_{1,3}-3_{1,2}$	52091.16	−0.11		
$4_{2,3}-3_{2,2}$	50792.00	0.02	49738.22	−0.08
$4_{2,2}-3_{2,1}$	50849.09	0.06		
$4_{3,2}-3_{3,1}$			49753.56	0.12
$4_{3,1}-3_{3,0}$			49753.56	−0.05
$10_{1,9}-10_{1,10}$	35873.22	0.02	34457.75	0.02
$11_{1,10}-11_{1,11}$	43015.69	0.07	41320.64	0.04
$12_{1,11}-12_{1,12}$			48789.98	−0.02
$20_{2,18}-20_{2,19}$	36387.15	−0.09	33841.98	−0.03
$21_{2,19}-21_{2,20}$	43045.46	−0.00	40084.22	−0.01
$22_{2,20}-22_{2,21}$			46982.48	0.02
b-Type				
$6_{0,6}-5_{1,5}$			22860.38	0.06
$7_{0,7}-6_{1,6}$	39032.13	−0.08	36924.13	−0.04
$8_{2,7}-9_{1,8}$			42606.56	0.04
$14_{1,13}-13_{2,12}$	42254.95	0.08		
$11_{2,9}-12_{1,12}$	46057.43	−0.05	47974.14	−0.03
$12_{2,10}-13_{1,13}$	39387.93	−0.03	41266.60	−0.02
$13_{2,11}-14_{1,14}$			35279.70	0.01
$15_{2,13}-16_{1,16}$	24170.42	0.00		
$16_{2,14}-17_{1,17}$	20856.49	0.01		
$17_{2,15}-18_{1,18}$	18490.10	0.04		
$25_{2,23}-26_{1,26}$	35775.54	−0.07		
$26_{2,24}-27_{1,27}$	42429.71	0.05		
$16_{3,14}-17_{2,15}$	49501.90	0.06		
$17_{3,15}-18_{2,16}$			39721.87	−0.02
$18_{3,15}-19_{2,18}$	49063.16	−0.01		
$19_{3,16}-20_{2,19}$	38754.06	−0.00	43228.79	0.02
$22_{2,20}-21_{3,19}$	34967.22	−0.01		
$25_{4,22}-26_{3,23}$	47248.50	−0.08		
$26_{4,22}-27_{3,25}$	49029.94	0.10		
$27_{4,23}-28_{3,26}$	36938.99	−0.04		

[a] Transition frequencies corrected for quadrupole coupling interaction are listed as observed values. [b] $\Delta = \nu_{obs} - \nu_{calc}$.

A series of $J_{0,J}-(J-1)_{1,J-1}$ transitions are strong, but they show only broadened spectral features. The transitions with resolved hyperfine structure have advantages for the first search even though they are weak as compared with those that show no hyperfine structure. The spectra due to naturally occurring ^{37}Cl species were found in a similar way.

For both isotopic species, the freqeuncies of all the observed transitions are listed in Table IV together with the calculated value fitted by a least-squares method. The best fit rotational and centrifugal distortion constants are listed in Table V. The quadrupole coupling constants of the Cl atom were determined by the least-squares fitting of the hyperfine splittings of $1_{0,1}-0_{0,0}$, $2_{1,2}-1_{1,1}$, and $2_{1,1}-1_{1,0}$ transitions of the normal species. The determined constants are listed in Table V together with calculated values. In the course of analysis the quadrupole interaction due to the nitrogen atom was neglected.

The dipole moment was determined from the Stark effect of the hyperfine components of $1_{0,1}-0_{0,0}$ with an applied electric field of 200–1200 V/cm. Methods applicable to the intermediate field case[9] were used for the analysis, since the frequency shifts were not proportional to the square of the electric field strength due to the large nuclear quadrupole interaction. The electrode spacing was calibrated using the Stark effect of the OCS $J = 2 \leftarrow 1$ transition and its dipole moment of 0.71521 D.[10] The determined dipole moment components are listed in Table V.

1-Azetine. According to the ab initio calculation based on the 4-31G(N*) basis set, 1-azetine is a nearly oblate symmetric top molecule and a-type transitions are considerably stronger than b-type transitions. In the survey spectra, four series of transitions were found in 33–45 GHz. The two stronger series were identified as a-type Q-branch $J_{J-2,3}-J_{J-4,4}$ and $J_{J-3,3}-J_{J-3,4}$ transitions, while the weaker series were identified as b-type Q-branch $J_{J-2,3}-J_{J-3,4}$ and $J_{J-3,3}-J_{J-4,4}$ transitions. The a- and b-type $J = 1 \leftarrow 0$ transitions were identified in the 20-GHz region from their characteristic Stark pattern. Other transitions were easily found with the predicted frequencies calculated by refined rotational constants. The observed frequencies are given in Table VI, and the rotational and centrifugal distortion constants determined by a least-squares fit are listed in Table VII.

Some of the transitions with small J showed triplets due to the nuclear quadrupole interaction of the nitrogen atom. The quadrupole coupling constants were determined from a least-squares fit of the hyperfine splittings of $1_{0,1}-0_{0,0}$, $2_{2,1}-2_{0,2}$, $2_{1,1}-2_{1,2}$, $3_{2,2}-3_{0,3}$, $3_{2,2}-3_{1,3}$, $3_{1,2}-3_{1,3}$, and $3_{1,2}-3_{0,3}$. The determined values are listed in Table VII for comparison with the calculated values. The dipole moment was determined, as given in Table VII, from the Stark effect of $1_{0,1}-0_{0,0}$ and $1_{1,1}-0_{0,0}$.

2-Azabutadiene. Since 2-azabutadiene has a large μ_b component according to ab initio MO calculation, a series of strong b-type Q-branch transitions were expected in the region higher than 43 GHz. In the survey spectra, strong transitions were found in 44855, 46053, and 47521 MHz, which were later identified as $4_{1,3}-4_{0,4}$, $5_{1,4}-5_{0,5}$, and $6_{1,5}-6_{0,6}$. Transitions with $J = 1$, 2, 3, and 7 were also easily found in the spectra. Most of these transitions exhibit approximate doublets due to the nuclear quadrupole interaction of the nitrogen atom. Since a nitrogen atom has nuclear spin $I = 1$, the transitions have three hyperfine components, two of which nearly coincide with each other.

In the next stage of the analysis, the b-type R-branch transitions $8_{0,8}-7_{1,7}$ and $9_{0,9}-8_{1,8}$ were searched for in the neighborhood of predicted transition frequencies. They were identified by their hyperfine structures, which were in good agreement with the predicted ones. Many b-type transitions and some a-type transitions were observed, and the frequencies are listed in Table VIII. The rotational, centrifugal distortion, and nuclear quadrupole coupling constants and dipole moment determined by least-squares fits are given in Table IX.

The nuclear quadrupole coupling constants were determined from many b-type transition and $2_{1,1}-1_{1,0}$, but they were not well determined since these transitions showed only partly resolved hyperfine structures. The dipole moment was determined from the Stark effect of $1_{1,0}-1_{0,1}$ and $2_{1,1}-2_{0,2}$.

Table V. Molecular Constants of *N*-Chloromethylenimine[a] (in MHz, u·Å^2, and D)

	$CH_2N^{35}Cl$ obs	$CH_2N^{35}Cl$ calc	$CH_2N^{35}Cl$ ρ[b]	$CH_2N^{37}Cl$ obs	$CH_2N^{37}Cl$ calc	$CH_2N^{37}Cl$ ρ[b]
A	62434.90 (10)	66532	1.065	62344.73 (11)	66435	1.066
B	6676.389 (13)	6769	1.014	6531.700 (13)	6622	1.014
C	6022.843 (11)	6144	1.020	5904.017 (11)	6022	1.020
Δ	0.11942 (22)	0.00		0.11970 (23)	0.00	
Δ_J	0.00403 (13)			0.00387 (10)		
Δ_{JK}	−0.0160 (33)			−0.0157 (20)		
Δ_K	1.587 (28)			1.576 (17)		
δ_J	0.0005167 (59)			0.0004858 (50)		
δ_K	0.02736 (23)			0.0269 (14)		
μ_a	1.873 (8)	1.95	1.04			
μ_b	1.441 (11)	1.90	1.32			
μ_c		0.0				
χ_{aa}(Cl)	−72.7 (4)	−68.2	0.94			
χ_{bb}(Cl)	30.1 (6)	28.0	0.93			
χ_{cc}(Cl)	42.6 (5)	40.2	0.94			
χ_{aa}(N)		3.61				
χ_{bb}(N)		−5.32				
χ_{cc}(N)		1.71				

[a] Numbers in parentheses represent 3 times the standard deviation attached to the last digits. [b] ρ = calc/obs.

Discussion

The main pyrolysis product of *N*-chloroazetidine was found to be *N*-chloromethylenimine. Recently, Amatatsu et al.[11] also have found *N*-chloromethylenimine and ethylene as pyrolysis products of the same precursor by infrared spectroscopy. These facts show that the main pathway of thermal decomposition of both *N*-chloroazetidine and azetidine is a ring cleavage. The situation

(9) Sugie, M.; Takeo, H.; Matsumura, C. *Bull. Chem. Soc. Jpn.* **1978**, *51*, 3065–3066.

(10) Muenter, J. S. *J. Chem. Phys.* **1968**, *48*, 4544–4547.

(11) Amatatsu, Y.; Hamada, Y.; Tsuboi, M., private communication.

Table VI. Transition Frequencies of 1-Azetine (MHz)

transition	ν_{obs}[a]	Δ[b]	transition	ν_{obs}[a]	Δ[b]
		a-Type			
$1_{0,1}-0_{0,0}$	19968.85	0.07	$8_{5,3}-8_{5,4}$	36911.98	0.04
$2_{2,1}-2_{0,2}$	20146.15	0.05	$9_{7,3}-9_{5,4}$	45048.27	0.04
$2_{1,1}-2_{1,2}$	16376.31	0.04	$9_{6,3}-9_{6,4}$	33598.75	0.02
$2_{1,1}-1_{1,0}$	45396.14	−0.06	$10_{8,2}-10_{8,3}$	9628.52	0.03
$2_{1,2}-1_{1,1}$	34478.70	−0.01	$10_{8,3}-10_{6,4}$	48151.45	−0.06
$2_{0,2}-1_{0,1}$	35500.12	−0.07	$10_{7,3}-10_{7,4}$	29487.57	0.03
$3_{2,2}-3_{0,3}$	30407.76	0.01	$11_{8,3}-11_{8,4}$	24827.88	0.00
$3_{1,2}-3_{1,3}$	29533.51	0.04	$11_{7,4}-11_{7,5}$	47575.12	−0.01
$3_{1,3}-2_{1,2}$	49484.33	−0.05	$12_{9,3}-12_{9,4}$	19931.29	0.00
$3_{0,3}-2_{0,2}$	49644.37	0.08	$12_{8,4}-12_{8,5}$	43863.62	0.01
$4_{4,1}-4_{2,2}$	26865.16	0.01	$13_{9,4}-13_{9,5}$	39155.67	0.01
$4_{3,1}-4_{3,2}$	12571.12	0.05	$14_{10,4}-14_{10,5}$	33683.32	0.03
$4_{2,2}-4_{2,3}$	28407.82	0.00	$15_{11,4}-15_{11,5}$	27782.85	0.02
$4_{2,3}-4_{0,4}$	42130.37	0.02	$16_{12,4}-16_{12,5}$	21842.96	−0.02
$5_{4,1}-5_{4,2}$	10135.23	0.04	$17_{12,5}-17_{12,6}$	43390.67	0.01
$5_{4,2}-5_{2,3}$	32124.68	−0.06	$18_{13,5}-18_{13,6}$	36660.92	0.05
$5_{3,2}-5_{3,3}$	26504.91	0.02	$19_{14,5}-19_{14,6}$	29677.07	−0.01
$5_{3,3}-5_{1,4}$	42077.24	0.08	$20_{15,5}-20_{15,6}$	22891.20	−0.04
$6_{6,1}-6_{4,2}$	40691.64	−0.03	$21_{15,6}-21_{15,7}$	46449.34	−0.04
$6_{5,2}-6_{3,3}$	34314.15	−0.00	$22_{16,6}-22_{16,7}$	38579.42	0.00
$6_{4,2}-6_{4,3}$	23848.34	0.04	$23_{17,6}-23_{17,7}$	30675.32	−0.02
$6_{4,3}-6_{2,4}$	42125.17	−0.01	$24_{18,6}-24_{18,7}$	23236.54	−0.02
$6_{3,3}-6_{3,4}$	40798.98	−0.02	$25_{18,7}-25_{18,8}$	48445.96	−0.07
$7_{5,2}-7_{5,3}$	20589.93	0.08	$26_{19,7}-26_{19,8}$	39569.04	−0.00
$7_{5,3}-7_{3,4}$	42443.02	0.00	$27_{20,7}-27_{20,8}$	30916.20	0.01
$7_{4,3}-7_{4,4}$	39296.29	0.02	$20_{21,7}-28_{21,8}$	23014.70	0.05
$8_{7,2}-8_{5,3}$	43451.14	−0.07	$29_{21,8}-29_{21,9}$	49481.47	−0.05
$8_{6,3}-8_{4,4}$	43294.83	0.01	$30_{22,8}-30_{22,9}$	39747.04	0.09
		b-Type			
$1_{1,1}-0_{0,0}$	21166.62	0.01	$9_{8,2}-9_{7,3}$	40939.52	−0.03
$2_{2,0}-2_{1,1}$	8030.69	−0.06	$9_{7,2}-9_{6,3}$	23218.32	0.02
$2_{0,2}-1_{1,1}$	34302.45	0.09	$9_{7,3}-9_{6,4}$	43625.86	−0.03
$2_{1,2}-1_{0,1}$	35676.52	−0.02	$9_{6,3}-9_{5,4}$	35021.08	0.01
$3_{3,0}-3_{2,1}$	10389.29	0.02	$10_{9,1}-10_{8,2}$	36366.68	0.04
$3_{2,2}-3_{1,3}$	30391.31	0.00	$10_{9,2}-10_{8,3}$	44851.18	−0.04
$3_{1,2}-3_{0,3}$	29549.94	0.03	$10_{8,2}-10_{7,3}$	25231.78	−0.00
$3_{0,3}-2_{1,2}$	49467.96	0.02	$10_{8,3}-10_{7,4}$	45090.74	−0.09
$3_{1,3}-2_{0,2}$	49660.70	−0.04	$11_{10,1}-11_{9,2}$	43357.90	0.03
$4_{4,1}-4_{3,2}$	24435.48	−0.05	$11_{10,2}-11_{9,3}$	49299.90	−0.07
$5_{5,0}-5_{4,1}$	18753.03	−0.07	$11_{9,2}-11_{8,3}$	28931.00	0.03
$5_{4,2}-5_{3,3}$	31681.43	−0.05	$11_{9,3}-11_{8,4}$	47197.61	−0.05
$5_{3,2}-5_{2,3}$	26948.18	0.03	$11_{8,3}-11_{7,4}$	30680.52	−0.02
$6_{6,0}-6_{5,1}$	24555.42	0.07	$11_{7,4}-11_{6,5}$	48196.60	0.04
$6_{5,2}-6_{4,3}$	33043.80	0.02	$12_{9,3}-12_{8,4}$	29997.11	−0.02
$6_{4,2}-6_{3,3}$	25118.72	0.05	$12_{8,4}-12_{7,5}$	45283.85	0.02
$6_{3,3}-6_{2,4}$	40854.76	−0.05	$13_{11,2}-13_{10,3}$	40817.57	0.00
$7_{7,0}-7_{6,1}$	30934.98	−0.00	$13_{10,3}-13_{9,4}$	30923.55	−0.07
$7_{7,1}-7_{6,2}$	35869.81	−0.06	$13_{9,4}-13_{8,5}$	42096.52	0.00
$7_{6,1}-7_{5,2}$	19710.30	0.04	$14_{12,2}-14_{11,3}$	48135.75	0.03
$7_{6,2}-7_{5,3}$	35015.37	−0.08	$14_{11,3}-14_{10,4}$	33696.63	0.03
$7_{5,2}-7_{4,3}$	23536.75	0.04	$14_{10,4}-14_{9,5}$	39233.68	−0.02
$7_{5,3}-7_{4,4}$	42243.10	−0.03	$15_{12,3}-15_{11,4}$	38340.42	0.05
$7_{4,3}-7_{3,4}$	39496.16	0.00	$15_{11,4}-15_{10,5}$	37367.07	−0.02
$8_{8,0}-8_{7,1}$	37465.36	−0.00	$16_{13,3}-16_{12,4}$	44617.48	0.07
$8_{8,1}-8_{7,2}$	40678.24	−0.04	$16_{12,4}-16_{11,5}$	37064.54	0.02
$8_{7,1}-8_{6,2}$	24086.32	−0.02	$17_{13,4}-17_{12,5}$	38695.08	−0.03
$8_{7,2}-8_{6,3}$	37646.42	−0.02	$18_{14,4}-18_{13,5}$	42402.39	0.02
$8_{6,2}-8_{5,3}$	22752.91	−0.02	$18_{13,5}-18_{12,6}$	45448.82	−0.04
$8_{6,3}-8_{5,4}$	42716.71	0.00	$19_{15,4}-19_{14,5}$	48071.04	0.07
$8_{5,3}-8_{4,4}$	37490.10	0.04	$19_{14,5}-19_{13,6}$	43850.92	−0.03
$9_{9,0}-9_{8,1}$	43872.93	0.03	$20_{15,5}-20_{14,6}$	44174.70	−0.01
$9_{8,1}-9_{7,2}$	29773.30	0.06	$21_{16,5}-21_{15,6}$	46706.12	−0.00

[a] Transition frequencies corrected for quadrupole coupling interaction are listed as observed values. [b] $\Delta = \nu_{obs} - \nu_{calc}$.

is different from the pyrolysis of the 3-membered ring systems, 2-methylaziridine and its chloride. In the pyrolysis of *N*-chloro-2-methylaziridine the dehydrochlorination occurs simultaneously with or in preference to a ring cleavage.

Hydrogen chloride was easily eliminated from *N*-chloroazetidine by *t*-BuOK, and 1-azetine was produced. The efficiency of dehydrochlorination was high when the reagent *t*-BuOK was kept at about 80 °C. In contrast, the dehydrochlorination of *N*-chloro-2-methylaziridine was unsuccessful. This is the second discrepancy between 4- and 3-membered ring systems.

The pyrolysis of 1-azetine gave an unstable molecule 2-aza-1,3-butadiene. According to the ab initio MO calculation on the basis of 4-31G(N*) basis set, the cis conformer is 0.0086 au (5.4 kcal/mol) less stable than the trans conformer. In fact the cis conformer could not be found in spite of a careful search.

In the course of analysis of spectra, the hyperfine structure was very useful for the assignment of transitions. Transitions having hyperfine structure have disadvantages since the peak intensity

Table VII. Molecular Constants of 1-Azetine[a] (in MHz, u·Å², and D)

	obs	calc	ρ[b]
A	13911.630 (24)	14078	1.012
B	12713.799 (24)	12918	1.016
C	7254.990 (24)	7350	1.013
Δ	−6.41874 (25)	−6.26	
Δ_J	0.0084 (16)		
Δ_{JK}	−0.012820 (63)		
Δ_K	0.00461 (29)		
δ_J	−0.0002322 (37)		
δ_K	−0.000174 (75)		
μ_a	2.203 (9)	2.26	1.03
μ_b	0.909 (12)	1.13	1.24
μ_c		0.0	
χ_{aa}	−2.75 (22)	−3.20	1.16
χ_{bb}	−0.38 (26)	−0.62	1.63
χ_{cc}	3.13 (15)	3.82	1.22

[a] Numbers in parentheses represent 3 times the standard deviation attached to the last digits. [b] ρ = calc/obs.

Table VIII. Transition Frequencies of 2-Azabutadiene (MHz)

transition	ν_{obs}[a]	Δ[b]	transition	ν_{obs}[a]	Δ[b]
		a-Type			
$1_{0,1}-0_{0,0}$	9316.69	0.09	$4_{3,2}-3_{3,1}$	37274.02	0.01
$2_{0,2}-1_{0,1}$	18629.51	0.02	$4_{3,1}-3_{3,0}$	37274.02	−0.10
$2_{1,1}-1_{1,0}$	19089.61	−0.03	$5_{0,5}-4_{0,4}$	46509.10	−0.00
$3_{0,3}-2_{0,2}$	27935.00	0.00	$5_{1,5}-4_{1,4}$	45425.66	0.01
$3_{1,2}-2_{1,1}$	28632.17	0.08	$5_{1,4}-4_{1,3}$	47707.44	0.07
$3_{2,2}-2_{2,1}$	27949.90	0.02	$5_{2,4}-4_{2,3}$	46574.73	0.07
$3_{2,1}-2_{2,0}$	27964.56	−0.02	$5_{2,3}-4_{2,2}$	46648.04	−0.02
$4_{0,4}-3_{0,3}$	37229.39	−0.03	$12_{1,11}-12_{1,12}$	35504.87	0.05
$4_{1,4}-3_{1,3}$	36346.04	−0.02	$13_{1,12}-13_{1,13}$	41381.46	0.01
$4_{1,3}-3_{1,2}$	38171.75	0.08	$22_{2,20}-22_{2,21}$	33225.32	−0.01
$4_{2,3}-3_{2,2}$	37263.55	0.01	$23_{2,21}-23_{2,22}$	38623.52	−0.02
$4_{2,2}-3_{2,1}$	37300.20	−0.07			
		b-Type			
$1_{1,0}-1_{0,1}$	42755.61	0.00	$22_{2,20}-23_{1,23}$	12833.12	0.03
$2_{1,1}-2_{0,2}$	43215.70	−0.05	$23_{2,21}-24_{1,24}$	14764.84	0.00
$3_{1,2}-3_{0,3}$	43912.76	−0.08	$24_{2,22}-25_{1,25}$	17409.90	−0.06
$4_{1,3}-4_{0,4}$	44855.12	0.03	$27_{2,25}-28_{1,28}$	29522.45	0.02
$5_{1,4}-5_{0,5}$	46053.31	−0.05	$28_{2,26}-29_{1,29}$	34901.38	0.02
$6_{1,5}-6_{0,6}$	47521.13	0.04	$29_{2,27}-30_{1,30}$	40918.35	−0.01
$7_{1,6}-7_{0,7}$	49274.16	0.00	$30_{2,28}-31_{1,31}$	47550.05	−0.00
$6_{0,6}-5_{1,5}$	16563.03	0.02	$16_{3,14}-17_{2,15}$	44456.10	−0.00
$7_{0,7}-6_{1,6}$	27072.17	−0.01	$17_{3,15}-18_{2,16}$	32925.27	−0.02
$8_{0,8}-7_{1,7}$	37725.89	0.02	$19_{3,17}-20_{2,18}$	8965.77	0.03
$9_{0,9}-8_{1,8}$	48501.89	−0.03	$22_{2,20}-21_{3,19}$	16207.25	−0.03
$7_{2,6}-8_{1,7}$	44958.04	−0.00	$23_{2,21}-22_{3,20}$	29240.42	−0.03
$8_{2,7}-9_{1,8}$	33654.50	−0.00	$24_{2,22}-23_{3,21}$	42560.15	−0.02
$9_{2,8}-10_{1,9}$	22145.88	0.00	$22_{3,19}-23_{2,22}$	12529.94	0.01
$10_{2,9}-11_{1,10}$	10437.44	−0.01	$18_{3,15}-19_{2,18}$	41978.68	0.01
$13_{1,12}-12_{2,11}$	13553.33	0.02	$19_{3,16}-20_{2,19}$	34183.04	0.05
$14_{1,13}-13_{2,12}$	25820.44	0.01	$21_{3,18}-22_{2,21}$	19425.52	0.03
$15_{1,14}-14_{2,13}$	38256.68	0.02	$27_{2,26}-26_{3,23}$	10976.76	0.00
$9_{2,7}-10_{1,10}$	48420.25	−0.02	$30_{2,29}-29_{3,26}$	23237.05	0.00
$10_{2,8}-11_{1,11}$	42304.31	0.01	$31_{2,30}-30_{3,27}$	26097.11	0.02
$11_{2,9}-12_{1,12}$	36630.75	0.00	$26_{4,22}-27_{3,25}$	45318.39	−0.00
$12_{2,10}-13_{1,13}$	31435.72	0.01	$27_{4,23}-28_{3,26}$	36299.78	−0.01
$13_{2,11}-14_{1,14}$	26755.67	0.01	$28_{4,24}-29_{3,27}$	27397.04	0.00
$14_{2,12}-15_{1,15}$	22626.50	−0.02	$29_{4,25}-30_{3,28}$	18630.98	0.02
$15_{2,13}-16_{1,16}$	19082.59	−0.07	$30_{4,26}-31_{3,29}$	10024.44	0.01
$16_{2,14}-17_{1,17}$	16155.90	−0.02	$25_{4,22}-26_{3,23}$	45981.29	−0.00
$17_{2,15}-18_{1,18}$	13874.75	0.02	$26_{4,23}-27_{3,24}$	34846.12	−0.01
$18_{2,16}-19_{1,19}$	12263.39	0.02	$27_{4,24}-28_{3,25}$	23446.02	0.00
$19_{2,17}-20_{1,20}$	11341.46	0.01	$28_{4,25}-29_{3,26}$	11759.46	−0.02
$20_{2,18}-21_{1,21}$	11123.59	0.01	$31_{3,28}-30_{4,27}$	12549.99	0.03
$21_{2,19}-22_{1,22}$	11619.27	−0.00			

[a] Transition frequencies corrected for quadrupole coupling interaction are listed as observed values. [b] $\Delta = \nu_{obs} - \nu_{calc}$.

Table IX. Molecular Constants of 2-Azabutadiene[a] (in MHz, u·Å², and D)

	obs	calc	ρ^b
A	47186.010 (23)	49086	1.040
B	4886.5325 (27)	4926	1.008
C	4430.0673 (23)	4477	1.011
Δ	−0.053877 (82)	0.00	
Δ_J	0.000995 (11)		
Δ_{JK}	−0.00801 (29)		
Δ_K	0.3406 (32)		
δ_J	0.00011743 (46)		
δ_K	0.005158 (51)		
μ_a	0.443 (33)	0.42	0.95
μ_b	1.896 (74)	1.64	0.86
μ_c		0.0	
χ_{aa}	0.5 (10)	0.92	1.84
χ_{bb}	−4.4 (11)	−5.14	1.17
χ_{cc}	3.9 (5)	4.22	1.08

[a] Numbers in parentheses represent 3 times the standard deviation attached to the last digits. [b] ρ = calc/obs.

becomes weaker, owing to the existence of hyperfine components. However, hyperfine splitting is useful for spectral assignment if the frequency shifts of the hyperfine components can be estimated with sufficient reliability. In case of a chlorine atom, the quadrupole coupling constants have been estimated empirically, since a cylindrical electron distribution around the bond that connects the chlorine with other atoms may be a good approximation. On the other hand, it is difficult to predict the quadrupole coupling constants of such atoms as nitrogen and boron. Recently, ab initio MO calculations have been able to give reliable molecular constants such as geometry, dipole moments, force field, electronic energy, and so on. Yamanouchi et al.[8] extended the program HONDOG so that it may give quadrupole coupling constants by the use of calculated field gradients. The calculated quadrupole coupling constants have been found to be in good agreement with experimental values.[8,12] The quadrupole coupling constants estimated by ab initio calculation are reliable enough to help the identification of transitions as described in the preceding section.

The ab initio MO calculation based on 4-31G(N*) or larger basis set gives sufficiently reliable geometrical parameters of midsized molecules, although it gives slightly shorter bond lengths since the SCF calculation neglects the effects of electron correlation.[13] The discrepancy comes partly from the experimental limitations. For most of molecules the r_0 or r_s structures are determined experimentally since it is impossible or extremely laborious to determine the equilibrium structures. In fact, the ab initio calculation gives rotational constants slightly larger than the experimental constants. Since the discrepancy lies between 1 and 4% in most cases, the discrepancy between calculated and experimental bond length is estimated to be less than 2%. The present study revealed that not only molecular geometry and electronic energy but also such molecular constants as dipole moments and hyperfine coupling constants can be calculated reliably by ab initio MO methods.

Acknowledgment. We are grateful to Dr. Peter A. Hackett for critical reading of the manuscript.

Registry No. 9, 32115-53-0; **10**, 32360-82-0; **11**, 6788-85-8; **12**, 382369-27-9; $CH_2N^{37}Cl$, 118017-56-4.

(12) Sugie, M.; Takeo, H.; Matsumura, C. *J. Mol. Spectrosc.* **1985**, *111*, 83-92.
(13) Pople, J. A. *Applications of Electronic Structure Theory*; Schaefer, H. F., III, Ed., Plenum: New York, 1977; Chapter 1.

Orientation of NH_3D^+ in Tutton Salt: Equilibrium Orientation and Tunneling Kinetics

Andrew P. Trapani[†] and Herbert L. Strauss*

Contribution from the Department of Chemistry, University of California, Berkeley, California 94720. *Received July 5, 1988*

Abstract: The equilibrium orientation and the kinetics of reequilibration of NH_3D^+ dilute in ammonium cobalt sulfate have been studied as a function of temperature. The equilibrium distribution has been examined by a Monte Carlo simulation and seems to correspond to a partially ordered orientational glass at temperatures below 20 K. To study the kinetics, the orientation distribution is perturbed either by T-jump or by laser spectral hole-burning in the infrared. The kinetics of the reequilibration of the various perturbed distributions are analyzed to find the rate constants for the different elementary reorientation processes of the NH_3D^+ ions. These rate constants show the temperature dependences characteristic of tunneling reactions. These include the range of possibilities from temperature independence to high-power-of-temperature dependence.

I. Introduction

Tunneling is a fundamental part of many chemical rate processes.[1,2] A number of different types of tunneling play a role in chemistry—particularly electron tunneling and nuclear or molecular tunneling. We consider only molecular tunneling in which a group of atoms penetrates through a barrier. Such tunneling has two well-known signatures: the presence of a large kinetic isotope effect and a characteristic temperature dependence. The temperature dependence shows a decreasing activation energy as the temperature is lowered and finally becomes nonexponential or even independent of temperature. It is the low-temperature dependence we have been able to demonstrate for a number of different reactions involving the NH_3D^+ ion dilute in the Tutton salt ammonium cobalt sulfate $[(NH_4)_2Co(H_2O)_6(SO_4)_2$, ACS]. A NH_3D^+ ion can exist in four crystallographically well-defined orientations (i.e., the N–D in one of the four approximately tetrahedrally placed directions) in the ACS crystal. The equilibrium distribution of the NH_3D^+ in these ions in the crystal changes with temperature,[3,4] and we can change the orientation

[†] Current address: Rohm & Haas Co. Research Laboratories, Spring House, PA 19477.

(1) Bell, R. P. *The Tunnel Effect in Chemistry*; Chapman and Hall: London, 1980.
(2) Goldanskii, V. I.; Fleurov, V. N.; Trakhtenberg, L. I. *Sov. Sci. Rev., Sect. B* **1987**, *9*, 59-124.
(3) Trapani, A. P.; Strauss, H. L. *J. Chem. Phys.* **1986**, *84*, 3577-3579.

0002-7863/89/1511-0910$01.50/0